# Highly Sensitive Fluorescence Probes for Organic Vapors: On/off and Dual Color Fluorescence Switching

**Byeong-Kwan An, Soon-Ki Kwon,† and Soo Young Park***

*Organic Nano-Photonics Lab., School of Materials Science & Engineering, Seoul National University, Seoul 151-744, Korea*
**E-mail: parksy@snu.ac.kr*
*†School of Nano & Advanced Materials and ERI, Gyeongsang National University, Jinju 660-701, Korea*
*Received March 21, 2005*

High-performance fluorescent probes which exhibit either on/off or dual color fluorescence switching in response to the presence of organic vapors with a rapid response, a high sensitivity and a high-contrast on/off signaling ratio were demonstrated on the basis of the vapor-controlled AIEE phenomenon.

**Key Words :** Fluorescent probe, Volatile organic compounds (VOCs), Chemosensor, Aggregation-induced enhanced emission (AIEE)

## Introduction

Fluorescent probe molecules that change their fluorescence intensities or wavelengths in response to the presence of volatile organic compounds (VOCs) have attracted much attention for developing practical chemosensor applications (ultimately for an artificial or electronic nose).[1] Most previous vapor sensor arrays using organic fluorescence probe materials rely upon solvatochromic events accompanying with fluorescence wavelength changes depending on the nature of the solvent vapor polarity.[2] Recently, transition-metal complexes of platinum(II) and gold (I) have also gained particular interest as fluorescent probe materials owing to their salient fluorescence modulation originating from the altered chemical interactions and crystal lattice structure upon sorption of organic vapors.[3] As an alternative and similarly effective fluorescent probe for organic vapors, we have recently considered a new class of organic molecules comprising a tunable molecular twist which exhibits the aggregation-induced enhanced emission (AIEE) in the solid state as well as the vapor-induced fluorescence quenching.[4] Herein we report the seminal high-performance fluorescent probes for the facile detection of organic vapors which exhibit either on/off or dual color fluorescence switching based on the vapor-controlled AIEE phenomenon.

Two different fluorescent probe molecules, 1-cyano-*trans*-1,2-*bis*-(4'-methylbiphenyl)ethylene (CN-MBE) and 4,4'-*bis*-((2-((4-(3,5-bitolyl)phenyl)phenyl)-2-cyano)-*trans*-ethenyl)-*trans*-stilbene (BPPCES) (Figure 1) for the on/off and dual color fluorescence switching in response to organic vapors, respectively, were investigated in this work. CN-MBE was synthesized as reported earlier,[4] while BPPCES was newly synthesized and characterized in this work.

CN-MBE and BPPCES molecules adsorbed on silica gel TLC plates[5] were prepared to ensure facile and effective access of small vapor molecules. Characteristic fluorescence switching of these plates was observed under 365 nm illumination at room temperature. CN-MBE and BPPCES molecules adsorbed on the TLC plate exhibited greenish blue and bright yellowish orange emission, which changed to the off and green emission, respectively, in the presence of dichloromethane vapors (Figure 1).

The vapor detection capability of CN-MBE and BPPCES was monitored to be fast and reversible under the dynamic condition where the flow of dichloromethane vapors carried by nitrogen gas (0.5 NL/min (L/min at 20 °C and 1 atm)) was turned on and off repeatedly. Figure 2(a) shows the actual spectral changes accompanying the on/off fluores-

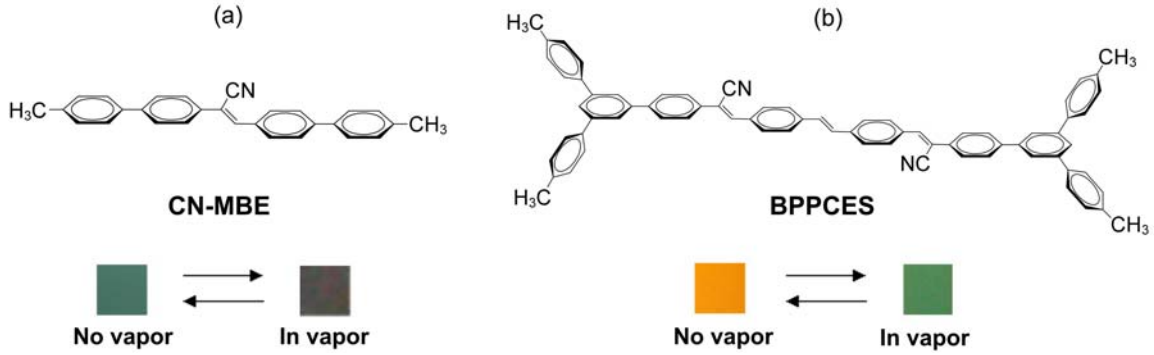


**Figure 1**. Chemical structures of CN-MBE (a) and BPPCES (b). The photos show fluorescence color changes of CN-MBE and BPPCES adsorbed on the silica TLC plate without vapor (left) and in vapor (dichloromethane) (right), respectively, under the 365 nm UV light illumination at room temperature.

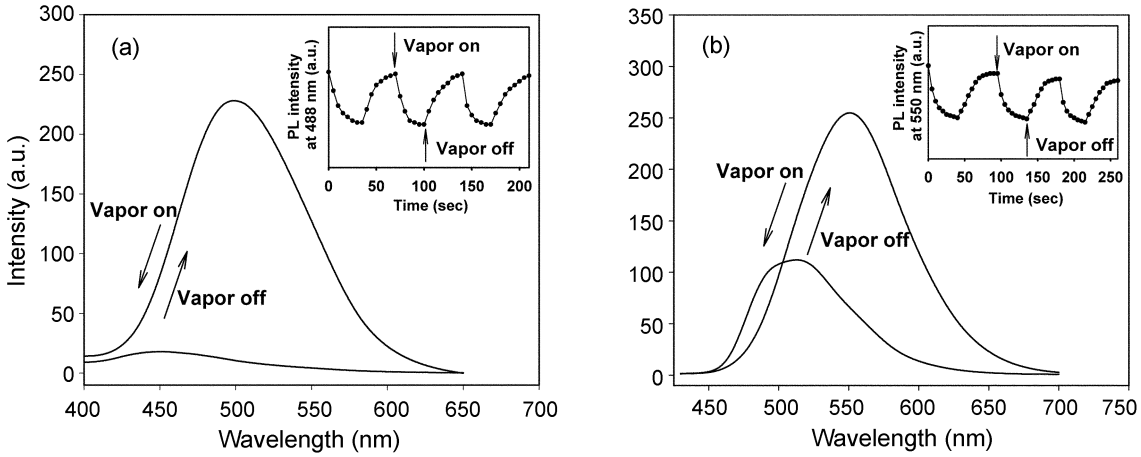


**Figure 2**. PL spectral changes of CN-MBE (a) and BPPCES (b) adsorbed on TLC plate depending on the on/off flow of dichloromethane vapors. Insets show PL intensity changes at 488 nm and 550 nm for CN-MBE and BPPCES, respectively.

cence switching of CN-MBE. In the absence of dichloromethane vapors, the maximum peak in the photoluminescence (PL) spectrum of CN-MBE is located around 488 nm, which gradually moves to the shorter wavelength with salient quenching of the PL intensity when the flow of dichloromethane vapors is switched on. It is noted that the overall PL intensity decreases by more than 24 times virtually resulting in the 'fluorescence off' state. However, the original blue emission around 488 nm of CN-MBE is completely restored when the flow of dichloromethane vapors is turned off subsequently. This reversible on/off fluorescence switching of CN-MBE is clearly depicted by the changes of PL intensity at 488 nm (Figure 2(a) inset). Figure 2(b) shows the dual color fluorescence switching of BPPCES modulated by the flow of dichloromethane vapors. In the absence of dichloromethane vapors, BPPCES shows a strong yellowish orange emission centered at around 550 nm. It changes, however, to the green emission centered at 512 nm with some decrease of PL intensity (< 60%) when the flow of dichloromethane vapor is turned on. The original yellowish-orange emission of BPPCES is also completely restored when the flow of dichloromethane vapors is turned off subsequently. This reversible dual color fluorescence switching of BPPCES is also clearly depicted by the changes of PL intensity at 550 nm (Figure 2(b) inset).

The selectivity of the fluorescent probes toward various organic solvent vapors[6] was examined by monitoring the fluorescence intensity changes ($I_0/I_{600}$ at 488 nm and 550 nm for CN-MBE and BPPCES, respectively) after 600s exposure in saturated vapors at 25 °C (Figure 3). It was noted that the vapors of good solvents for probe molecules like dichloromethane, chloroform and tetrahydrofuran showed extremely high sensing abilities ($I_0/I_{600}$ > 17 and 5 for CN-MBE and BPPCES, respectively). However, *n*-hexane, methanol and water vapors which are poor solvents for probe molecules exhibited poor fluorescence probing sensitivity. This result implies that the on/off and dual color fluorescence switching of CN-MBE and BPPCES are not attributed to the solvatochromic effect but to the solubilizing

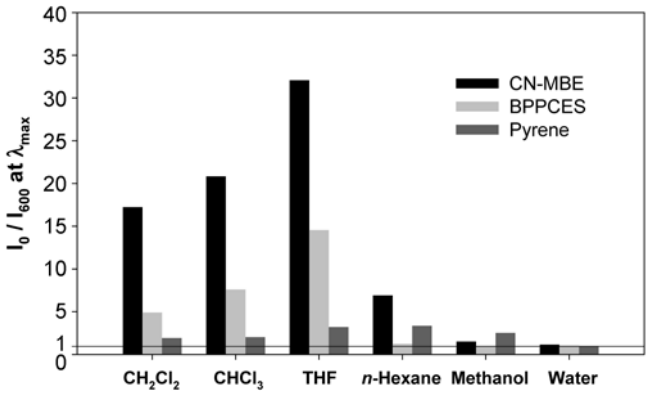


**Figure 3**. Fluorescence intensity changes of CN-MBE and BPPCES adsorbed on silica TLC plates after 600 sec exposure of the saturated vapors at the room temperature. $I_0$ is the initial intensity and $I_{600}$ is the intensity at 600 sec. Fluorescence intensity change of pyrene is also included for comparison.[7]

effect of organic vapors. It is most likely that the vapor molecules of good solvents are ready to isolate the AIEE molecules from the aggregated ones reversibly, which is necessarily accompanied by the dramatic fluorescence changes.

Drastic changes of the fluorescence emission intensity and wavelength of CN-MBE and BPPCES molecules upon exposure of organic vapors must be explained in terms of the changes of molecular conformation and specific intermolecular interactions. Both CN-MBE and BPPCES are considered to be significantly twisted in the isolated state due to the steric interactions in biphenyl units[8] as well as in the bulky cyano groups attached into vinylene moiety.[9] On the other hand, more planar and conjugated conformation of CN-MBE and BPPCES is favored in the aggregated state to augment the strong intermolecular forces against the intramolecular steric factors leading to the twisted conformation.[10] This aggregation-induced planarization extends the effective $\pi$-conjugation of CN-MBE and BPPCES and partly contributes to the fluorescence switch-on. It is also speculated that the bulky and polar cyano groups in CN-MBE and BPPCES play a decisive role of inducing a *J*-

aggregation instead of the more common face-to-face intermolecular interactions (*H*-aggregation).[11] As a result, combined effect of intramolecular planarization and *J*-aggregate formation lead to an enhanced emission and a bathochromic shift in the aggregated state, so-called aggregation-induced enhanced emission (AIEE) phenomenon.[12,13]

The postulated AIEE mechanism of CN-MBE and BPPCES was experimentally evidenced by the UV/vis absorption and PL spectra of CN-MBE and BPPCES in isolated THF solution and nanoparticle suspensions. Nanoparticle suspensions of CN-MBE and BPPCES ($2 \times 10^{-5}$ mol·L$^{-1}$) were prepared by a simple precipitation method (80 vol % water addition in THF solution) without surfactants for the quantitative comparison with the diluted THF solution of CN-MBE and BPPCES ($2 \times 10^{-5}$ mol·L$^{-1}$). The presence of nanoparticles was confirmed by FE-SEM (inset photos of (a) and (b) in Figure 4). The maximum peaks in the absorption spectra of both CN-MBE and BPPCES are red-shifted from the isolated molecules to the nanoparticles (Figure 4(a) and (b)). This bathochromic shift of the absorption peaks indicates that the effective conjugation lengths of CN-MBE and BPPCES are extended from isolated twisted molecule to the planar conjugated one in nanoparticles. Furthermore, the new shoulder bands around 420 and 480 nm of CN-MBE and BPPCES which are not observed in the dilute solution are assigned to the *J*-aggregation band of CN-MBE and BPPCES owing to the bulky and polar cyano groups which restrict the face-to-face intermolecular interactions. The tails from 500 nm of absorption spectra in THF/water mixture are attributed to Mie scattering caused by nanosized particles.[14]

The planarization and *J*-aggregation process of CN-MBE and BPPCES are more dramatically evidenced by the PL studies (Figure 4(c) and (d)). The fluorescence intensity of CN-MBE and BPPCES increases, and their emission maximum peaks are red-shifted from the dilute solution to the nanoparticles. The inset photographs of Figure 4(c) and (d) show that aggregated CN-MBE and BPPCES (nanoparticle suspension (N) and powder (P), respectively) are strongly fluorescent and orange fluorescence emission, respectively, while isolated CN-MBE and BPPCES in any kinds of solvents (benzene (B), chloroform (C), THF (T) and acetonitrile (A), respectively) is virtually non-fluorescent and green fluorescence emission, respectively. This result suggests that the AIEE phenomenon of CN-MBE and BPPCES in the aggregated state is not caused by the special solvatochromic effect but by the unique AIEE phenomena.

Based on this AIEE mechanism, the unique fluorescent

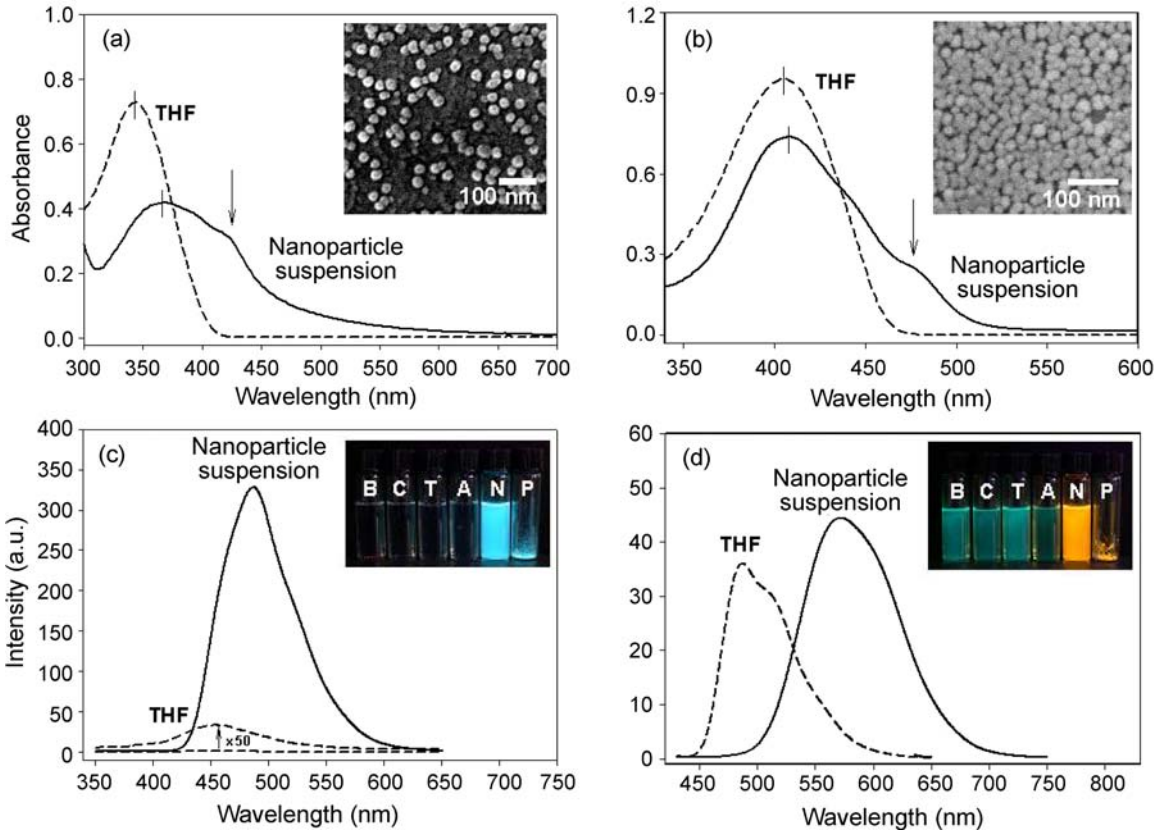


**Figure 4**. (a) and (b) UV/vis absorption of CN-MBE and BPPCES ($2 \times 10^{-5}$ mol·L$^{-1}$) in THF and nanoparticle suspension (THF/water mixture), respectively. The arrows ( ↓ ) indicate the *J*-aggregation band owing to the specific arrangements by cyano group. Inset photos show FE-SEM images of CN-MBE and BPPCES nanoparticles obtained from nanoparticles' suspension containing 80% volume fractions of water in THF. (c) and (d) PL spectra of CN-MBE and BPPCES ($2 \times 10^{-5}$ mol) in THF and nanoparticle suspensions, respectively. The PL intensities were normalized by the corresponding UV absorbance. The inset photos show the fluorescent emission of CN-MBE (c) and BPPCES (d) ($2 \times 10^{-5}$ mol·L$^{-1}$) in different solvents and solid state (B: benzene, C: chloroform, T: THF, A: acetonitrile, N: nanoparticle suspension, P: powder, respectively) under the 365 nm of UV light illumination.

probing capability of CN-MBE and BPPCES can be explained unambiguously. That is, the deformation of coplanarity and consequent fluorescence changes occur when small solubilizing vapor molecules penetrate into the free volume of the aggregated AIEE molecules because the vapor molecules weaken the intermolecular interactions and make the aggregated molecules locally isolated. During the vapor exposure, therefore, twisted conformation is generated and the effective $\pi$-conjugation lengths in CN-MBE and BPPCES are reduced bringing about the fluorescence quenching and blue-shifted emission, respectively. The original bright and red-shifted fluorescence emission of CN-MBE and BPPCES in the aggregated state are completely recovered when the vapor molecules are removed.

Because the vapor detection of CN-MBE and BPPCES probe molecules is fast, sensitive and reversible, small leakage flow of organic vapors from tubes or vessels can be monitored *in situ* as a real-time fluorescence image. Figure 5 shows the proof-of-concept photograph which images the flow of vapor leakage (*ca*. 0.5 mm size hole) as a fluorescence contrast.

In conclusion, we have demonstrated high-performance fluorescent probes for organic vapors using AIEE fluorophores, CN-MBE and BPPCES. Upon exposure to organic vapors, CN-MBE and BPPCES showed reversible on/off fluorescence and dual color fluorescence switching, respectively, with a rapid response, a high sensitivity and a high-contrast on/off signaling ratio. These reversible switching behaviors are attributed to the changes of the molecular conformation and intermolecular interactions in the sensing molecules by the penetration of the organic vapors. The simple sensing apparatus using CN-MBE and BPPCES absorbed on silica gel TLC sheets offered real-time vapor leak detections.

## Experimental Section

CN-MBE was prepared according to our previous method.[4] BPPCES was prepared by the synthetic route depicted in Scheme 1.

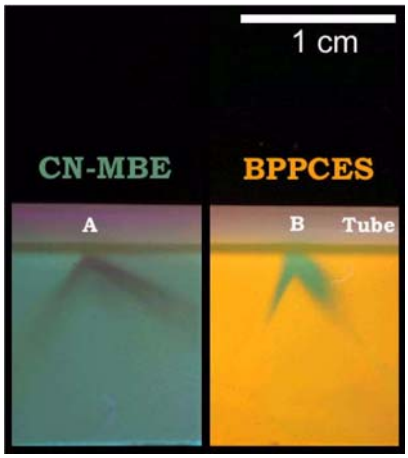


**Figure 5**. Proof-of-concept vapor leak detection using CN-MBE and BPPCES. **A** and **B** indicate the position of the leakages (*ca*. 0.5 mm size hole).

**1,3,5-Tri-*p*-tolyl-benzene (1) and 4,4'-dimethyl-*trans*-stilbene (2).** Compound **1** was prepared according to the literature[15] and compound **2** was purchased commercially.

**1,3-Bis-(*p*-tolyl)-5-(*p*-cyanomethyl-phenyl)-benzene (3).** *N*-Bromosuccinimide (NBS) (2.56 g, 14.4 mmol) was added to a solution of compound **1** (4.89 g, 14.4 mmol) in $CCl_4$ (100 mL) and the mixture was refluxed for 24 h. The mixture was poured into a 500 mL of water and stirred for 2 h. After the solvent was removed under vacuum, the residue was added into a solution of NaCN (2.35 g, 48.0 mmol) in tetrahydrofuran (THF) (50 mL). The mixture was stirred at 50 °C for 24 h. After cooling to room temperature, the resulting mixture was column chromatographed on silica gel, eluting with ethyl acetate/hexane (1 : 3 by volume) solvent. After removing solvent under vacuum, the solid product was obtained (2.04 g, 39% yield). $^1$H-NMR (300 MHz, $CDCl_3$) $\delta$ [ppm]: 7.76 (s, 1H, Ar-H), 7.72 (d, $J$ = 8.4 Hz, 4H, Ar-H), 7.60 (d, $J$ = 8.0 Hz, 4H, Ar-H), 7.45 (d, $J$ = 8.3 Hz, 2H, Ar-H), 7.30 (d, $J$ = 8.3 Hz, 4H, Ar-H), 3.81 (s, 2H, -$CH_2$CN), 2.46 (s, 6H, (-$CH_3$)$_2$). IR (KBr, cm$^{-1}$): 3010, 2950, 2250, 1600, 1500, 1410, 800. MS (EI) (calcd for $C_{28}H_{23}N$, 373.49; found, 373) *m/e*: 373, 318, 239, 186, 91.

***trans*-Stilbene-4,4'-dicarbaldehyde (4).** Bromination reaction of **2** (2.00 g, 9.6 mmol) was carried by the same procedure above. After bromination, the residue was added

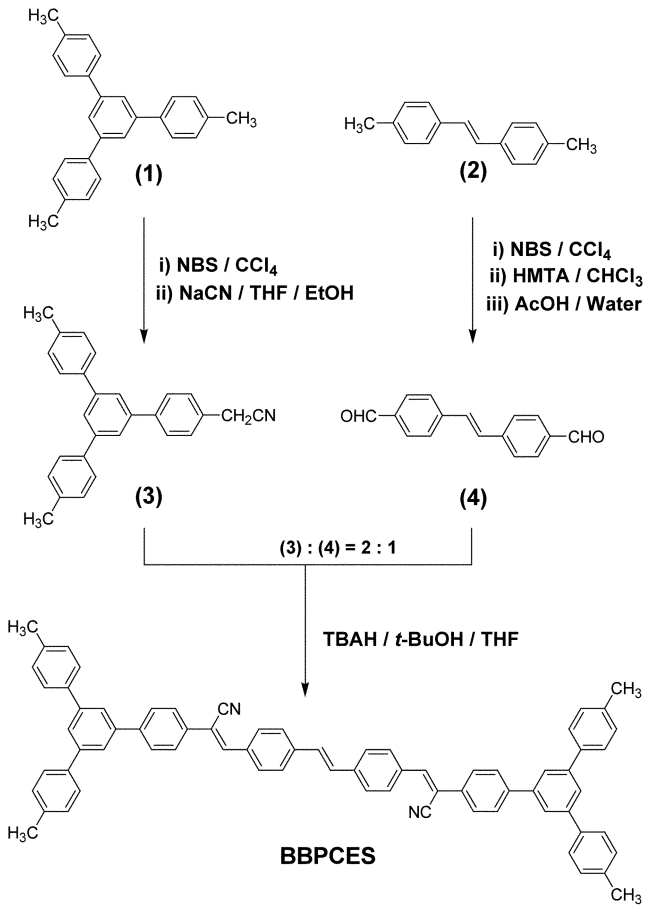


**Scheme 1**. Synthetic route of BPPCES.

into a solution of hexamethylenetetramine (HMTA) (4.00 g, 29.5 mmol) in chloroform (30 mL). The mixture was refluxed for 12 h. After cooling to room temperature, the solvent was removed under vacuum. 30 mL of glacial acetic acid (AcOH) and water mixture (1 : 1 by volume) was poured into the reaction mixture and refluxed for 2 h. The resulting mixture was column chromatographed on silica gel, eluting with ethyl acetate/hexane (1 : 3 by volume) solvent. After removing solvent under vacuum, the solid product was obtained (0.35 g, 15% yield). $^1$H NMR (300 MHz, $CDCl_3$) $\delta$[ppm]: 10.0 (s, 2H, -CHO), 7.89 (d, $J$ = 8.2 Hz, 4H, Ar-H), 7.68 (d, $J$ = 8.2 Hz, 4H, Ar-H), 7.30 (s, 2H, vinyl-H). MS (EI) (Calcd. for $C_{16}H_{12}O_2$: 236.27. Found: 236) *m/e*: 236, 207, 178, 152, 135, 89, 73, 44.

**4,4'-Bis-((2-((4-(3,5-bitollyl)phenyl)phenyl)-2-cyano)-*trans*-ethenyl)-*trans*-stilbene (BPPCES).** The mixture of **3** (0.40 g, 1 mmol) and **4** (0.13 g, 0.5 mmol) in *t*-butyl alcohol (5 mL) and THF (1 mL) was stirred at 50 °C for 1 h. Tetrabutylammonium hydroxide (TBAH) (1 M solution in methanol) (0.1 mL) was slowly dropped into the mixture and stirred for 1 h. The orange precipitate was collected by filtration and washed with methanol (0.47 g, 93% yield). $T_{\text{decomp (onset, 5 wt\% loss)}}$ = 401 °C. $^1$H NMR (300 MHz, $CDCl_3$) $\delta$ [ppm]: 7.98 (d, $J$ = 8.6 Hz, 4H, Ar-H), 7.78 (m, 14H, Ar-H), 7.64 (m, 15H, Ar-H), 7.32 (m, 9H, Ar-H), 2.43 (s, 12H, -$CH_3$). FT-IR (KBr, cm$^{-1}$): 3043, 2932, 2212 (-CN attached to vinylene), 1584, 1508, 1271, 812, 753. MS (FAB) (Calcd for $C_{72}H_{54}N_2$: 947.2. Found: 947.0) *m/e*: 947, 934, 820, 718, 613, 460, 307, 154, 136, 89, 39. Anal. Calcd $C_{72}H_{54}N_2$: C, 91.30; H, 5.75; N, 2.96. Found: C, 91.00; H, 5.75; N, 2.97.

**Instrumentation.** $^1$H NMR spectra recorded on a Jeol JNM-LA300 (300 MHz) in $CDCl_3$ solutions with $CHCl_3$ at 7.26 ppm as the internal standard. IR spectra were measured on a Midac FT-IR spectrophotometer using KBr pellets. Mass spectra were measured on a JMS AX505WA by EI mode. UV-visible absorption and fluorescence emission spectra were recorded on a HP 8452-A and a Shimadzu RF-500 spectrofluorophtometer, respectively. The fluorescence displays of CN-MBE and BPPCES on the TLC sheets were photographed on a Nikon-Coolpix 995 digital camera. PL intensities at 488 nm and 550 nm were monitored on a high-sensitivity Laser Power Meter (LaserMate/Q, COHERENT). FE-SEM images of CN-MBE and BPPCES nanoparticles were acquired on a JSM-6330F (JEOL) by dropping nano-particles' suspension on glass substrates.

**Acknowledgement.** This work was supported by the Ministry of Science and Technology of Korea through National Research Laboratory (NRL) program awarded to Prof. Soo Young Park. We are grateful for the instrumental support from the equipment facility of CRM-KOSEF, Korea University.

## References

1. (a) Prasanna de Silva, A.; Nimal Gunaratne, H. Q.; Gunnlaugsson, T.; Huxley, A. J. M.; McCoy, C. P.; Rademacher, J. T.; Rice, T. E. *Chem. Rev.* **1997**, *97*, 1515. (b) Albert, K. J.; Lewis, N. S.; Schauer, C. L.; Sotzing, G. A.; Stitzel, S. E.; Vaid, T. P.; Walt, D. R. *Chem. Rev.* **2000**, *100*, 2595. (c) Oh, D. J.; Han, M. S.; Kim, D. H. *Bull. Korean Chem. Soc.* **2004**, *25*, 1495.
2. (a) Dickinson, T. A.; White, J.; Kauer, J. S.; Walt, D. R. *Nature* **1996**, *382*, 697. (b) Walt, D. R.; Dickinson, T.; White, J.; Kauer, J.; Johnson, S.; Engelhardt, H.; Sutter, J. M.; Jurs, P. C. *Biosens. Bioelectron.* **1998**, *13*, 695. (c) Albert, K. J.; Walt, D. R. *Anal. Chem.* **2000**, *72*, 1947.
3. (a) Buss, C. E.; Mann, K. R. *J. Am. Chem. Soc.* **2002**, *124*, 1031. (b) Kato, M.; Omura, A.; Toshikawa, A.; Kishi, S.; Sugimoto, Y. *Angew. Chem. Int. Ed.* **2002**, *41*, 3183. (c) Fernández, E. J.; López-de-Luzuriaga, J. M.; Monge, M.; Olmos, M. E.; Pérez, J.; Laguna, A.; Mohamed, A. A.; Fackler, J. P. *J. Am. Chem. Soc.* **2003**, *125*, 2022. (d) Lu, W.; Chan, M. C. W.; Zhu, N.; Che, C.-M.; He, Z.; Wong, K.-Y. *Chem. Eur. J.* **2003**, *9*, 6155.
4. An, B.-K.; Kwon, S.-K.; Jung, S.-D.; Park, S. Y. *J. Am. Chem. Soc.* **2002**, *124*, 14410.
5. Silica gel TLC aluminum sheets were obtained from Merck (specific area (480-540 m$^2$/g), pore volume (0.74-0.84 mL/g), and layer thickness (175-225 mm)).
6. Selected organic solvents have a different dielectric constant ($\varepsilon$) (*e.g.*, dichloromethane ($\varepsilon$ = 8.93), chloroform ($\varepsilon$ = 4.81), tetrahydrofuran ($\varepsilon$ = 7.58), *n*-hexane ($\varepsilon$ = 1.88), methanol ($\varepsilon$ = 32.70), water ($\varepsilon$ = 80.10)) and a high volatility at room temperature.
7. For evaluating the excellent vapor sensing capability of CN-MBE and BPPCES molecules against conventional fluorescent probe materials, a pyrene which is one of the most widely used fluorescent probe molecules was chosen as a control whose vapor probing sensitivity and selectivity were measured under the same condition as CN-MBE and BPPCES. The excimer emission ($\lambda_{max}$ = 498 nm) of pyrene molecules adsorbed on silica gel TLC sheets decreased when exposed to solvent vapors most likely due to the increased distance between proximal pyrene molecules by the penetration of solvent vapors, leading to the restriction of the excimer formation.
8. Allmenningen, A.; Bastiansen, O.; Fernholt, L.; Cyvin, B. N.; Cyvin, S. J.; Samdal, S. *J. Mol. Struct.* **1985**, *128*, 59.
9. Lange, F.; Hohnholz, D.; Leuze, M.; Ryu, H.; Hohloch, M.; Freudenmann, R.; Hanack, M. *Synth. Met.* **1999**, *101*, 652.
10. It is well known that biphenyl and stilbene derivatives showed these conformational changes from the solution state to the solid state owing to the same reasons. (a) Ambrosch-Draxl, C.; Majewski, J. A.; Vogl, P.; Leising, G. *Phys. Rev. B* **1995**, *51*, 9668. (b) Brédas, J. L.; Thémans, B.; Fripiat, J. G.; André, J. M.; Chance, R. R. *Phys. Rev. B* **1984**, *29*, 6761. (c) Tian, B.; Zerbi, G.; Müllen, K. *J. Chem. Phys.* **1991**, *95*, 3198. (d) Woo, H. S.; Lhost, O.; Graham, S. C.; Bradley, D. D. C.; Friend, R. H.; Quattrocchi, C.; Brédas, J. L.; Schenk, R.; Müllen, K. *Synth. Met.* **1993**, *59*, 13.
11. Oelkrug, D.; Tompert, A.; Gierschner, J.; Egelhaaf, H.; Hanack, M.; Hohloch, M.; Steinhuber, E. *J. Phys. Chem. B* **1998**, *102*, 1902.
12. (a) An, B.-K.; Lee, D.-S.; Lee, J.-S.; Park, Y.-S.; Song, H.-S.; Park, S. Y. *J. Am. Chem. Soc.* **2004**, *126*, 10232. (b) Lim, S.-J.; An, B.-K.; Jung, S.-D.; Chung, M.-A.; Park, S. Y. *Angew. Chem. Int. Ed.* **2004**, *43*, 6346.
13. The similar phenomenon was also suggested by Tang *et al.* and Yang *et al.* (a) Luo, J.; Xie, Z.; Lam, J. W. Y.; Cheng, L.; Chen, H.; Qiu, C.; Kwok, H. S.; Zhan, X.; Liu, Y.; Zhu, D.; Tang, B. Z. *Chem. Commun.* **2001**, 1740. (b) Chen, J.; Xie, Z.; Lam, J. W. Y.; Law, C. C. W.; Tang, B. Z. *Macromolecules* **2003**, *36*, 1108. (c) Li, S.; He, L.; Xiong, F.; Li, Y.; Yang, G. J. *Phys. Chem. B* **2004**, *108*, 10887.
14. Auweter, H.; Haberkorn, H.; Heckmann, W.; Horn, D.; Lüddecke, E.; Rieger, J.; Weiss, H. *Angew. Chem. Int. Ed.* **1999**, *38*, 2188.
15. Elmorsy, S. S.; Pelter, A.; Smith, K. *Tetrahedron Lett.* **1991**, *32*, 4175.